BNL-113532-2017

Position-Sensitive Virtual Frisch-Grid (VFG) Gamma Ray Detectors for Safeguard Applications

Aleksey Bolotnikov

January 2017

Nonproliferation and National Security Department
Radiation Detector and Nonproliferation R&D Group

Brookhaven National Laboratory

U.S. Department of Energy
USDOE National Nuclear Security Administration (NNSA),
Office of Defense Nuclear Nonproliferation (NA-20)

DISCLAIMER

Position-sensitive virtual Frisch-grid (VFG) Gamma Ray Detectors for Safeguard Applications

Presented at the annual review
January 24th, 2017

Principal Investigator: Aleksey Bolotnikov
Point of Contact: Peter Vanier

BROOKHAVEN NATIONAL LABORATORY

a passion for discovery

Office of Science U.S. DEPARTMENT OF ENERGY

Research team

- BNL team: G. S. Camarda, Y. Cui, R. Gul, G. De Geronimo, J. Fried, A. Hossain, L. Ocampo, C. Salwen, E. Vernon, G. Yang, and R. B. James (SRNL)
- BNL students: M. Petryk, S. Cheng, A. McGilloway, C. Cherches, M. Siegel and R. Gallagher
- External Collaborator: FLIR Systems, Inc.
- Subcontractors: Redlen and eV Products

Introduction

- Goal: Incorporate an array of the novel position-sensitive virtual Frisch-grid CdZnTe detectors into the existing FLIR instrument (R200)
- Motivation: need for better gamma-ray detectors with enhance spectral resolution, efficiency and functionalities
- FLIR offers today three handheld instruments (all used by IAEA inspectors)

IdentiFINDER R400

NaI(Tl) scintillator
~6% at 662 keV

IdentiFINDER R300
(formerly nanoRAIDER**)**

Hemispherical CZT
detectors, 2-3% at 662 keV

IdentiFINDER R200
(recently introduced)

CsI scintillator
≤ 7.5% at 662 keV

We propose to upgrade this device because has the most recent DAQ and signal processing platform

These devices are compact, rugged, very reliable, have great functionality and convenient user interface but have limited spectral resolution

Goal - Integrate VFG detectors into FLIR R200

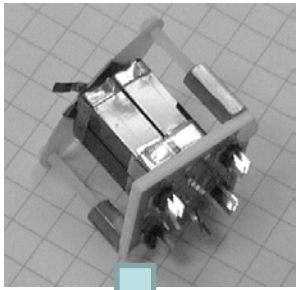

VFG Detectors

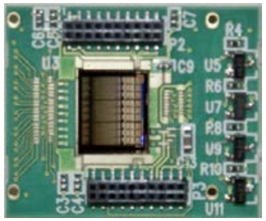

ASIC board
VGA1 ASIC

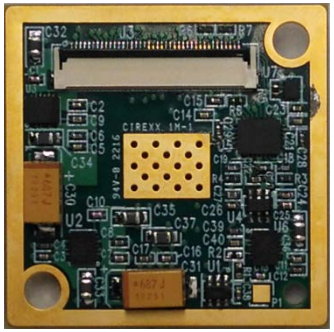

Adaptor Board

ASIC board plugged
into Adaptor Board

Short
cable

FLIR R200

Current status

- New adaptor board -- Complete
- We worked with FLIR closely on this project to make sure that the adaptor board will fit into R200 device -- Complete
- FLIR is to modify their acquisition board of R200 to the new VFG-based devices – Work in progress (FLIR is waiting for CRADA)
- A bridge board for testing the adaptor board with BNL’s acquisition system -- Complete
- The bridge board was used to test the adaptor and verify that it works as designed – Complete
- CRADA has been approved! (InCRADAble news)
- Preparation for testing the current prototype at SRNL (and eventually the first FLIR prototype) – In progress
- <u>Two new tasks:</u>
- Develop an algorithm for position reconstruction -- Complete
- Test a linear (1x6) array of VFG detectors -- Complete

Bridge board

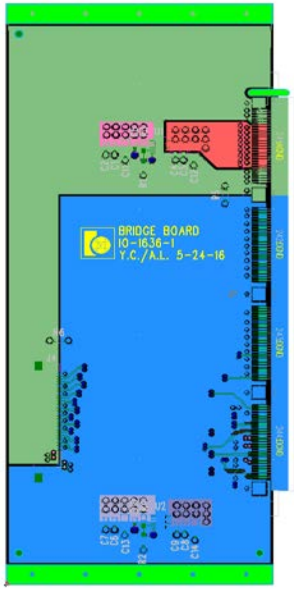

Examples of commonly used CZT detectors today

- Today, CZT detectors is a proven technology: high-efficiency, excellent energy and position resolutions, operate at ambient temperature
- They are particularly beneficial in compact handheld instruments for field applications
- However, crystal defects, which are present even in the best quality CZT crystals, affect production yield and increase cost of CZT detectors

Examples of large-volume CZT detectors available today

Hemispherical
15x15x10 mm^3

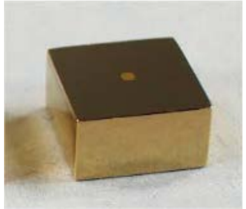

CPG
20x20x15 mm^3

- Typical energy resolution is 2-3% at 662 keV
- Drift-time correction

3D pixelated detectors
20x20x15 mm^3 1.7-mm pixels

eV Products

H3D

- Typical resolution 1-2%
- Best resolution: 0.5% at 662 keV using carefully selected CZT crystals

Detectors rely on the highest quality CZT crystals to achieve their best performances → Such crystals have low production yields and are very expensive! Maximum thickness is limited by 15 mm!

Arrays of virtual Frisch-grid (drift) detectors

- To overcome the high cost and low availability of big CZT crystals we propose arrays of small cross-section, up to 7x7 mm^2, but long, up to 5 cm, detectors
- Such crystals have much higher production-yield and lower; typically cut from the crystals rejected by other costumers
- The bars are configured as position-sensitive virtual Frisch-grid detectors:

Examples of CZT bars

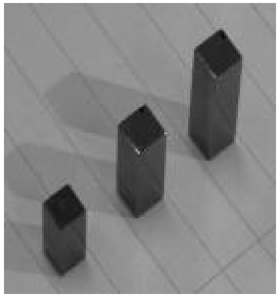

Position-sensitive virtual Frisch-grid detector

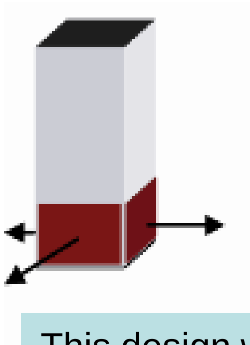

We attached 4 position-sensing pads (non-contacting electrodes) for measuring X-Y coordinates of interaction points

The cathode signals are used to measure drift times to evaluate Z coordinates, like in TPC

Virtually grounded pads produce the Frisch-grid effect (as if a real grid were placed inside the detector)

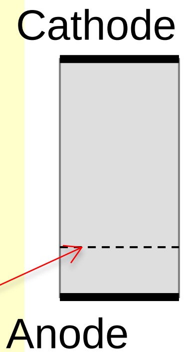

Can be used in large-area arrays or in small, 2x2, arrays that we proposed for FLIR instruments

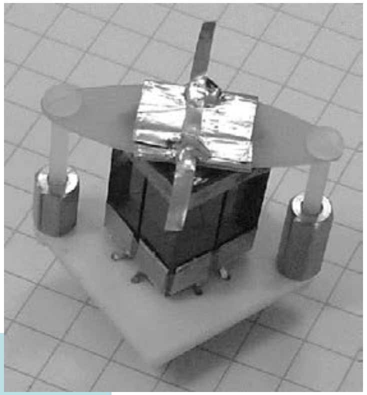

This design was originally proposed for noble gas detectors by V. Chernaytin et al. First applied to CZT detectors by G. Montemont (LETI) and D. McGregor (Kansas State University)

Virtual Frisch-grid effect produced by grounded pads

Pulse-height spectra measured with shielded and unshielded detectors

Unshielded detector

Detector with shielding pads

5x5x10 mm^3 detector

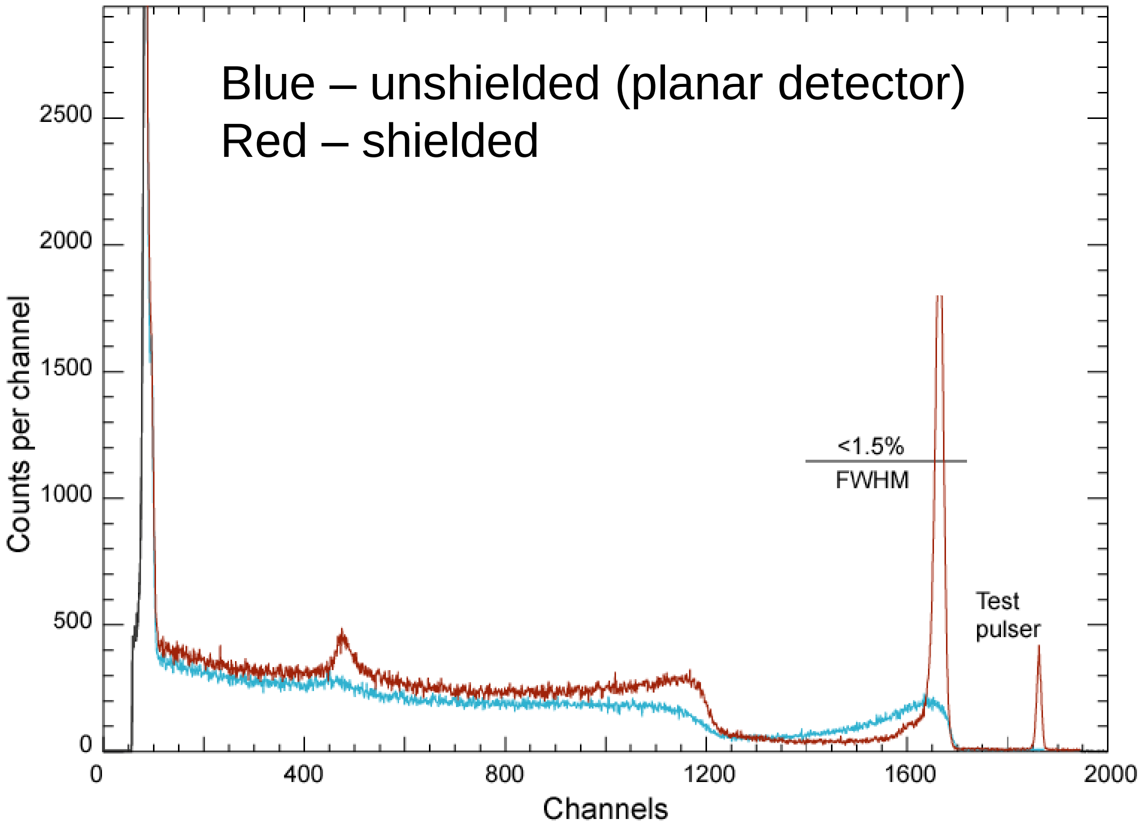

X-Y spatial resolution of position-sensitive virtual Frisch-grid detectors

6x6x15 mm^3 virtual Frisch-grid detector detector irradiated with a ^{241}Am source

Image of a 1-mm Tungsten slit collimator placed above the cathode

6x6 mm^2 area

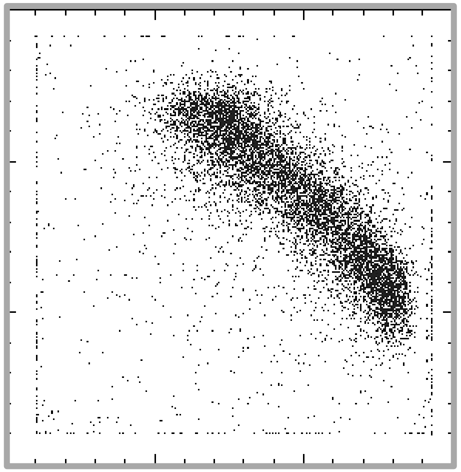

- High-resolution position sensing is the most important feature of our detectors
- It allows us to correct the detector response non-uniformities caused by crystal defects
- Benefits of this approach:
  - Employ unselected low-cost CZT crystals and, at the same time, achieve a high energy resolution
  - Use longer crystals (higher detection efficiency)
  - Operate detectors at lower biases

Position-sensitive virtual Frisch-grid detectors (CZT drift detectors)

3D position-sensitive device

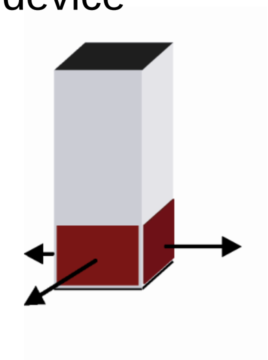

- Because defects locations are fixed, the response non-uniformity is caused by random distributions of interaction points → Such variations can be corrected if the locations of interaction points are known with sufficient accuracy
- Position information allows us to virtually segment a detector into small voxels and equalize responses from each voxel
- A 3D correction matrix (lookup table) is generated during calibration

Raw spectrum

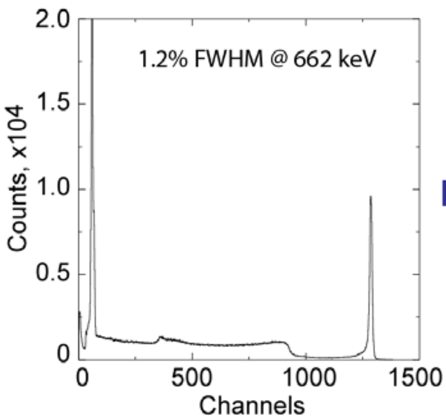

Responses from individual voxels

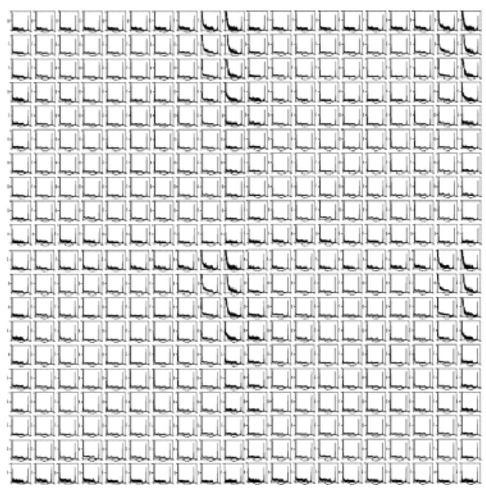

After equalizing responses from individual voxels

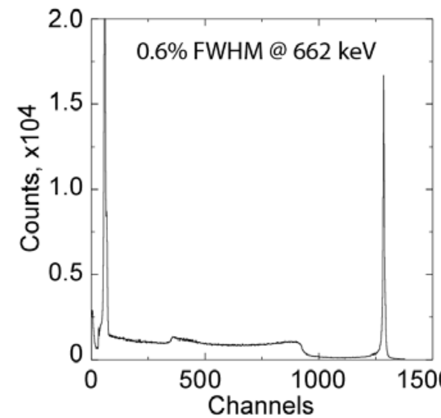

In practice, we need to generate a 3D response matrix (calibration step) and use it to correct measured signals

How we fabricate detectors and arrays

For insulation and mechanical protection of CZT crystals, we use the ultra-thin polyester shrink tube (Advanced Polymer, Inc.)

This material has very high dielectric strength and resistivity

Dielectric strength: > 4,000 V/mil
Volume Resistivity: 10^{18} Ohm-cm,
Surface Resistivity: 10^{14} Ohm/square,
Dielectric Constant: 3.3

A crystal and two aluminum bars are inserted inside the tube and put inside hot water (~80 C) for 2-3 min. The remaining tube is cut and edges are trimmed.

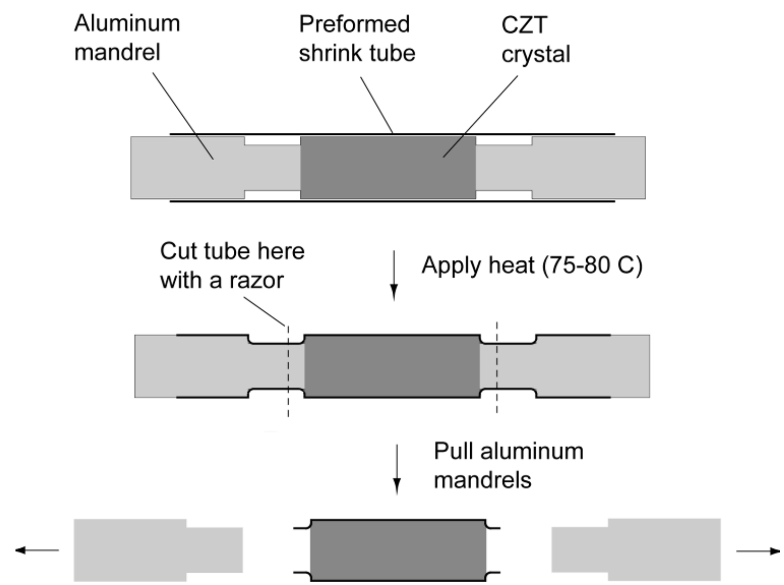

Encapsulated crystal inside the shrink tube

BROOKHAVEN NATIONAL LABORATORY

Experimental setup for testing virtual Frisch-grid detectors

Example of a 40-mm
thick detector

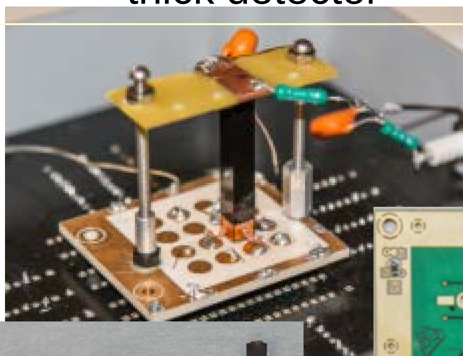

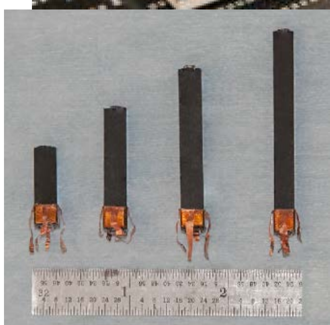

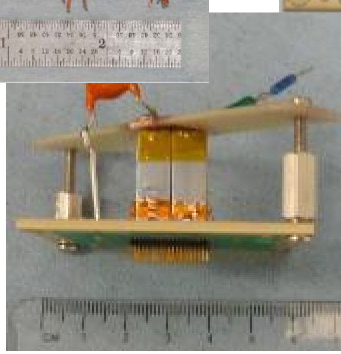

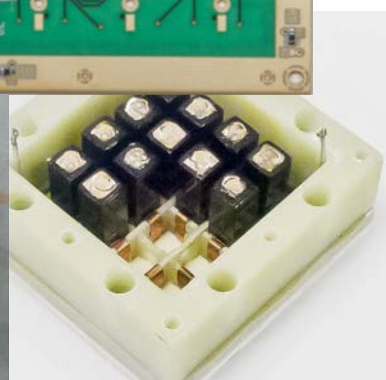

Detector
board

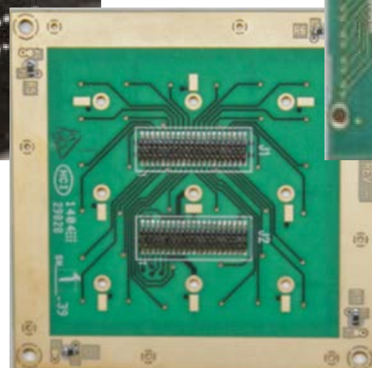

ASIC board

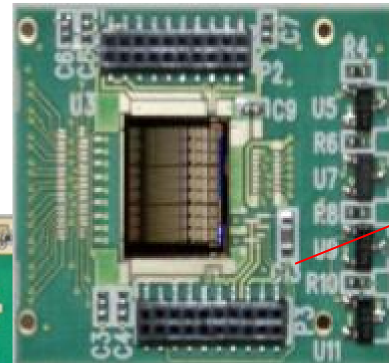

Test box

Currently, we employ the existing ASIC and DAQ developed for the conventional CZT arrays which has many limitations in the case of position-sensitive detectors

Its architecture is identical to the H3D ASIC developed by the BNL’s Instrumentation Division in collaboration with the University of Michigan

For the position-sensitive detector arrays we are currently developing the new ASIC which will be available next year

Typical charge signals (after preamps) generated on the cathode, anode, and sensing pads

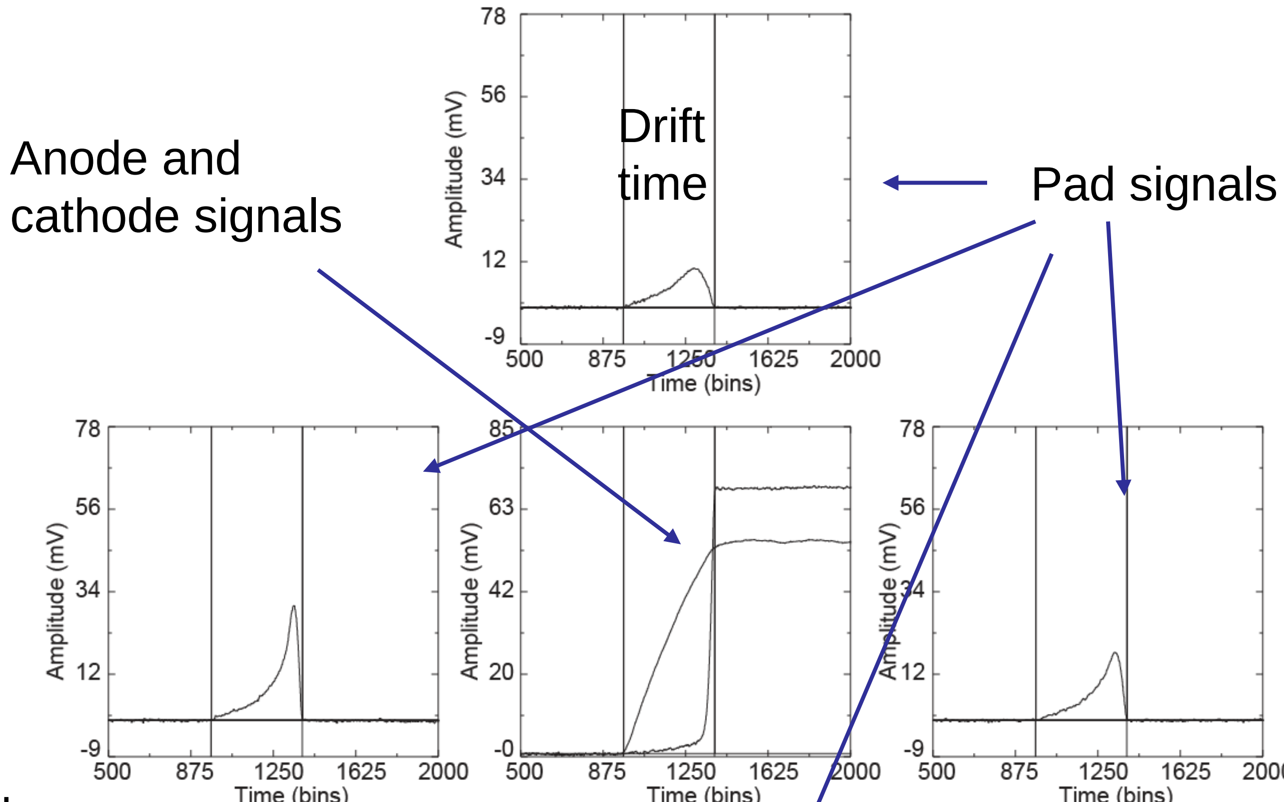

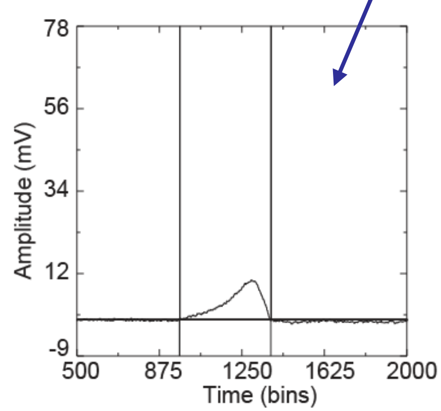

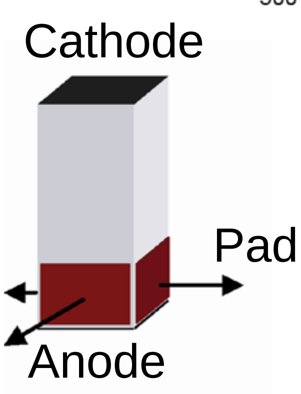

After unipolar shaping the pad signals have positive and negative components

The negative amplitude is independent from the interaction depth.

Pad signals can substitute for the cathode signals!

Testing a 4x4 array prototype (NA22 project)

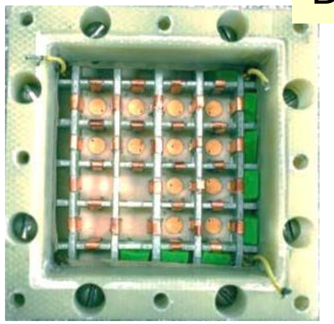

Detectors housing

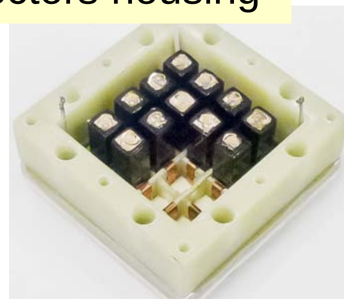

Test box

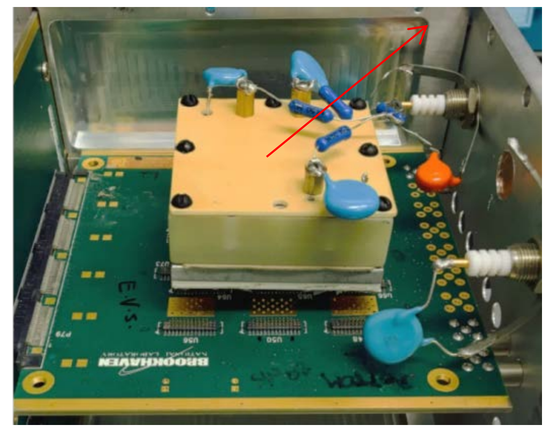

Pad connections in
a 4x4 module

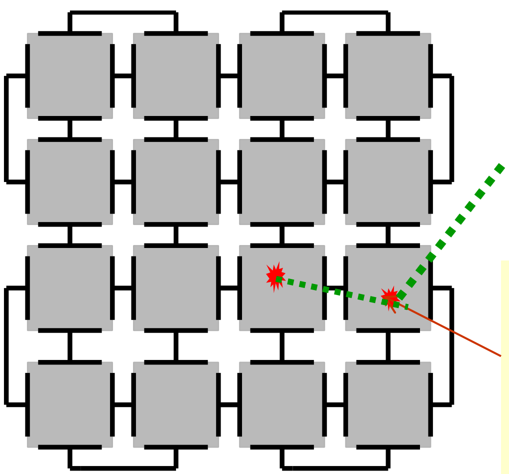

Incident
photon

Ambiguity
problem in the
case of
multiple
interaction
points

16 anodes
4 cathodes
32 sensing pads

Best results from 20, 30, 40,and 50 mm thick detectors

Raw spectra | 3D correction | FWHM maps | Selected areas

20 mm

30 mm

40 mm

50 mm

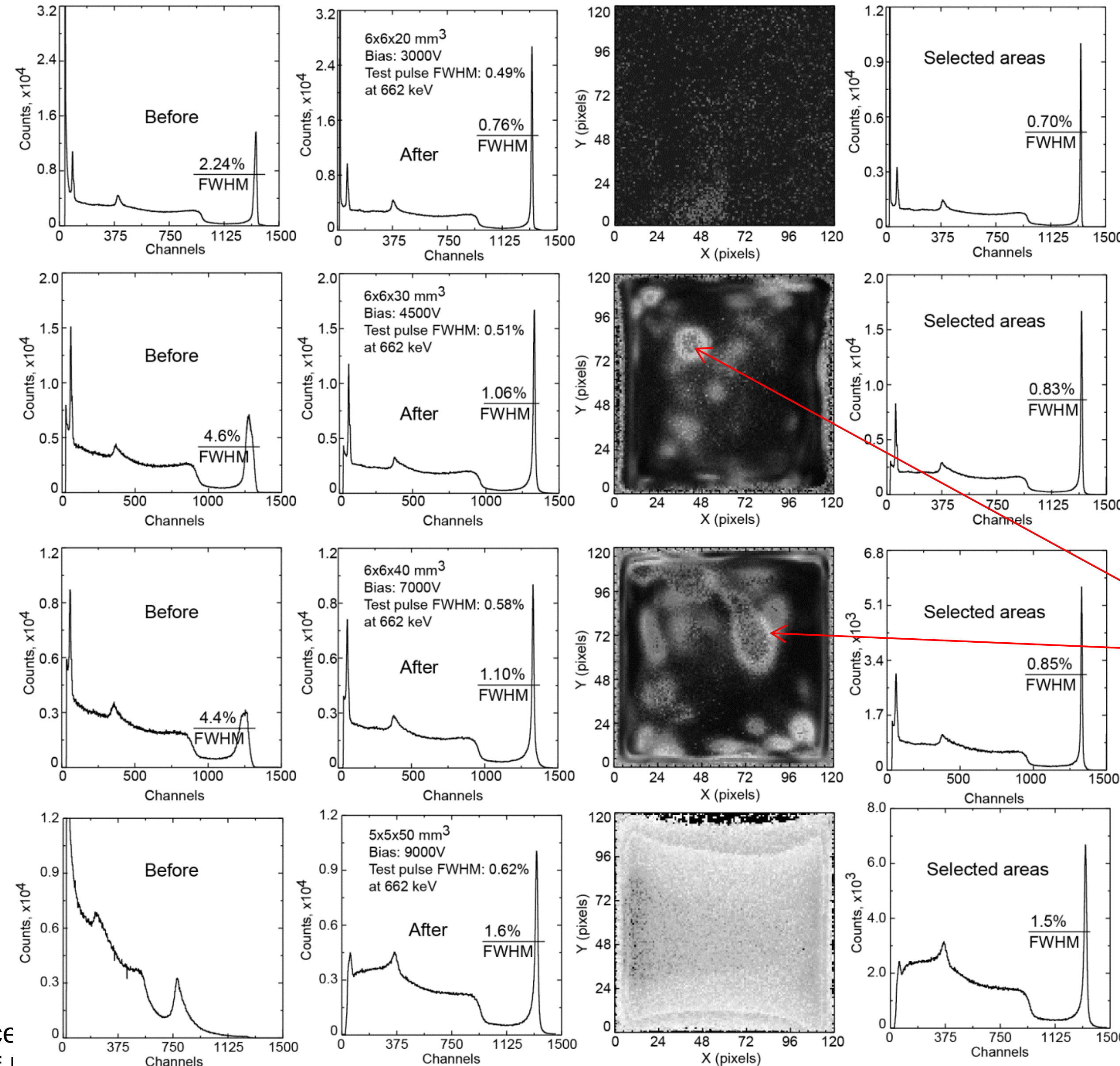

^{137}Cs source

Prismatic defects

BROOKHAVEN NATIONAL LABORATORY

We can correct full spectra (not a single gamma-line)

7x7x20 mm^3 Redlen crystal

Cathode bias 3000 V

Improvement of spectral response after 3D corrections

Temperature: 17 C

The energy resolution is limited by the electronic noise

Before

After

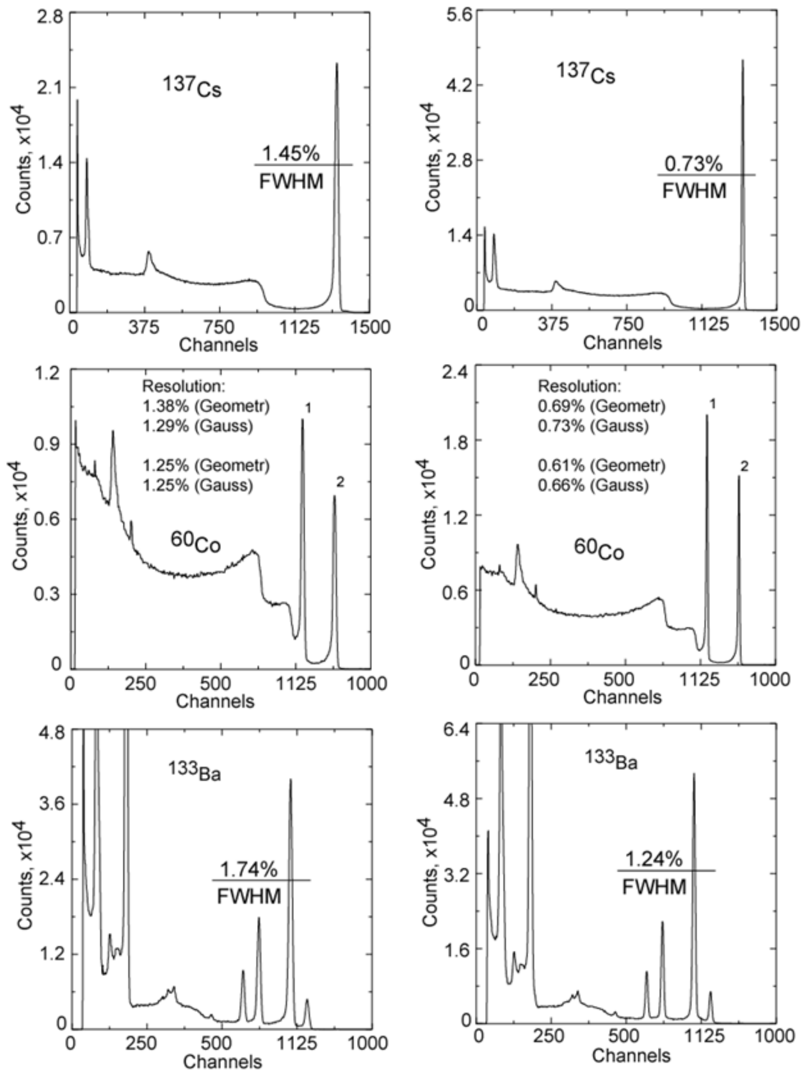

^{137}Cs

^{60}Co

^{133}Ba

Broad energy range

Increased efficiency allows detection of energetic gamma rays

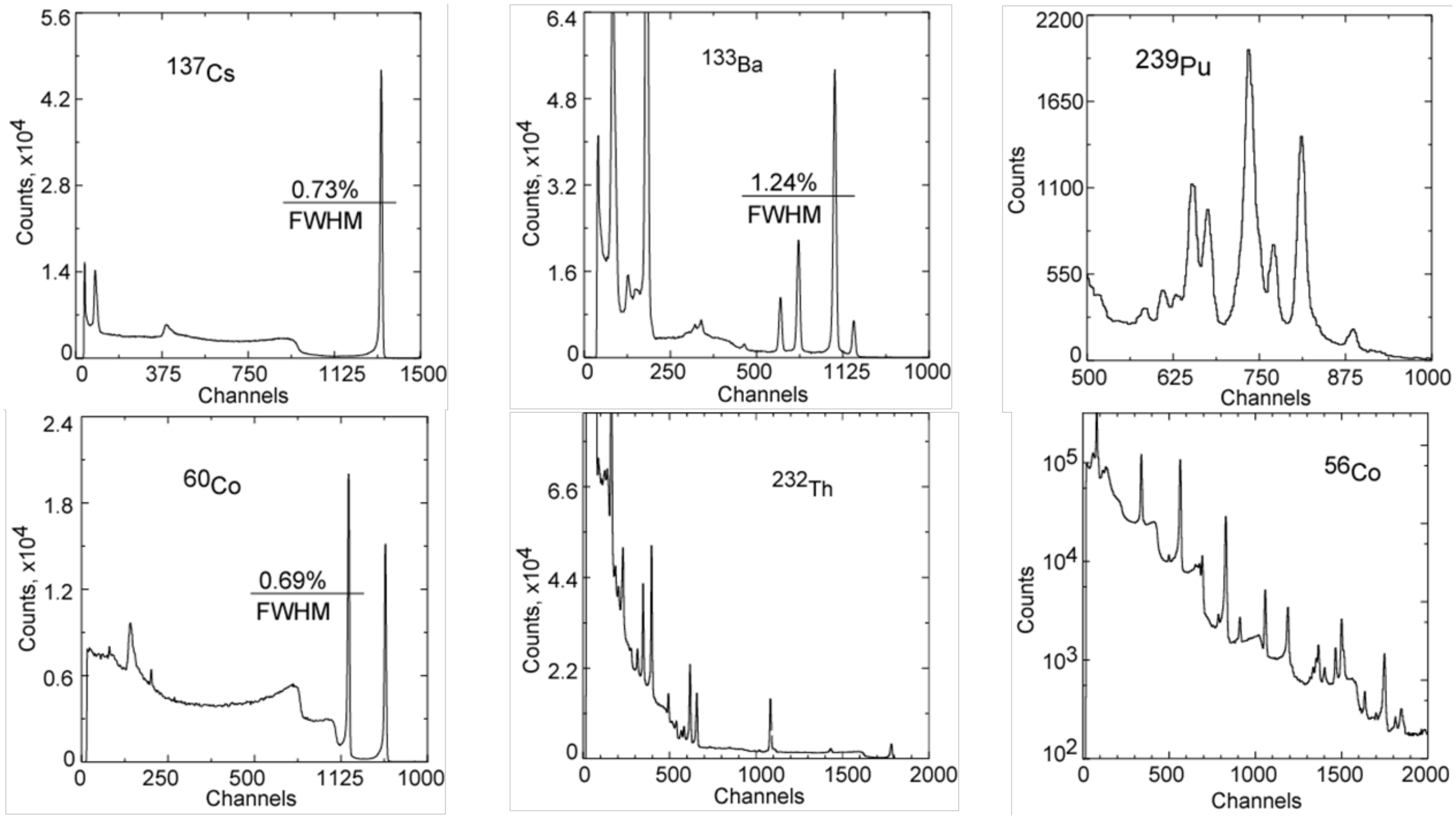

Pu-239

6x6x20 mm^3 position sensitive detector

Before

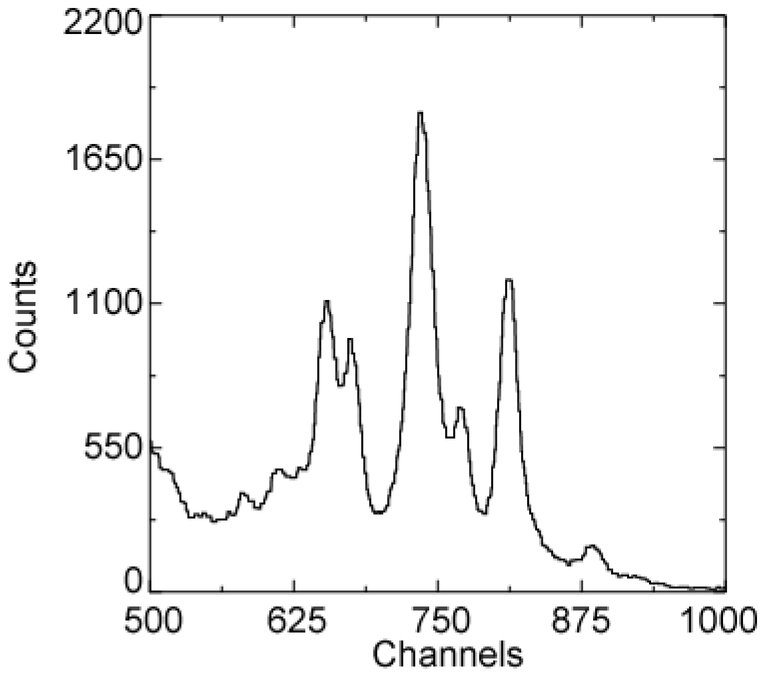

After

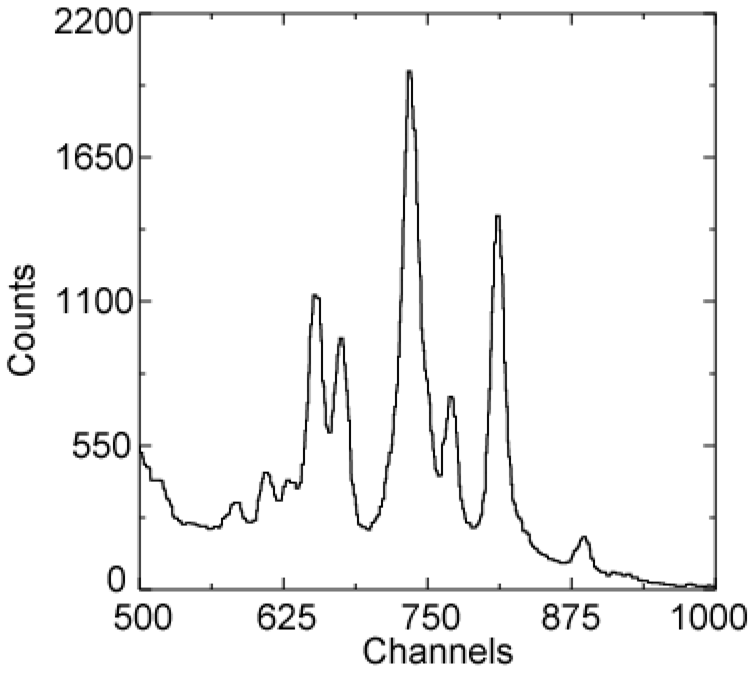

We can make thicker detectors biased at lower voltages

Dependence of energy resolution
vs. applied bias measured for
a 20-mm-thick detector

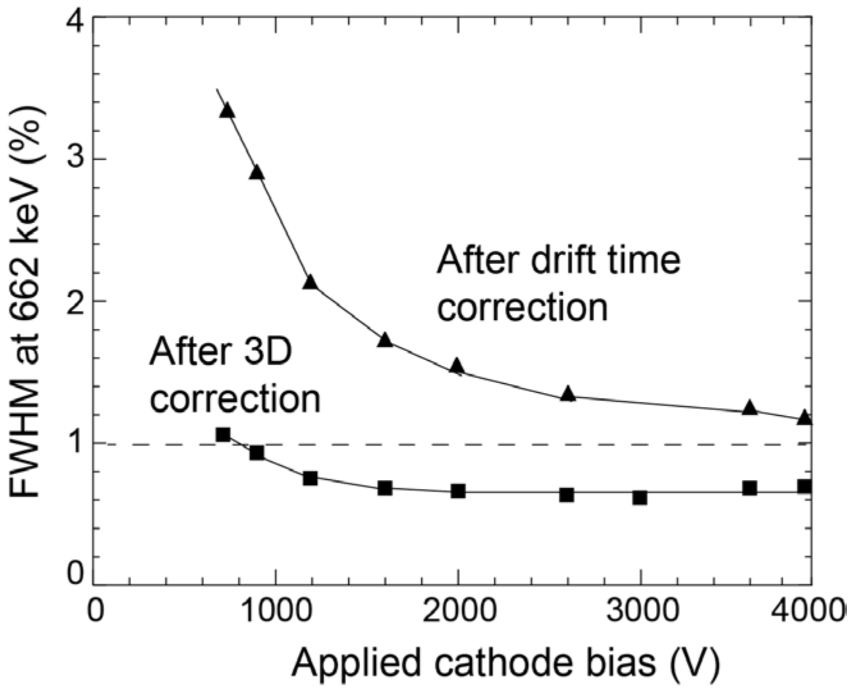

Can operated at reduced bias but the electric field must be above a certain limit (~1000 V/cm) to attain <1% resolution (~2500 V/cm in pixel detectors)

Temperature dependence of energy resolution

20-mm long detector
Bias 3000 V

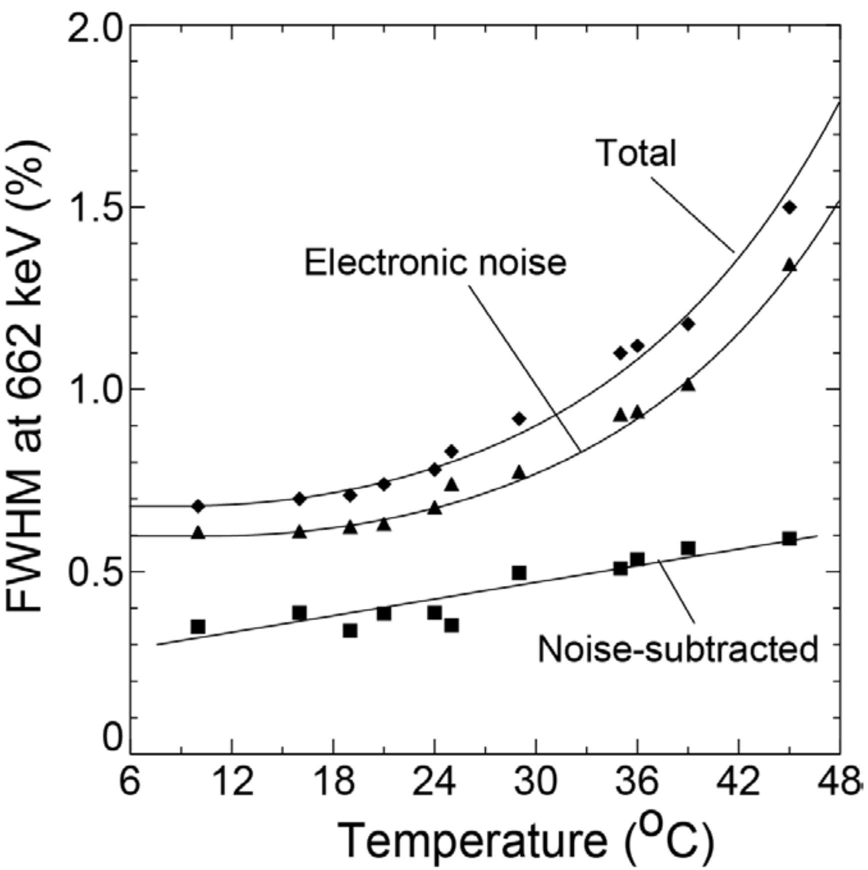

Correction matrixes were evaluated at each temperature

Energy resolution is primarily limited by the electronic noise (leakage current)

Position sensing

Schematic of a position-sensitive VFG detector

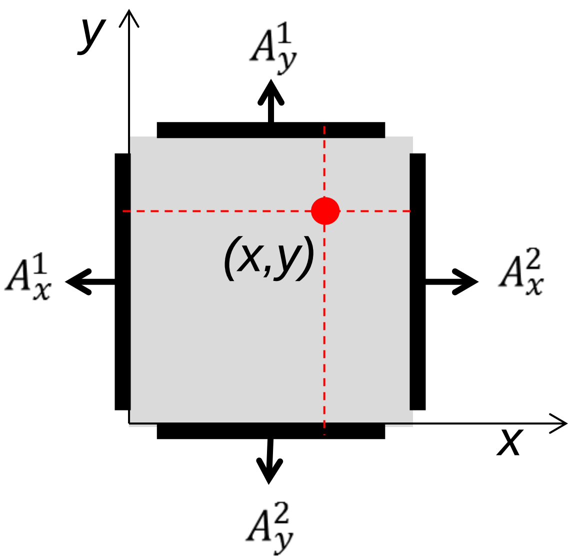

If assume a linear approximation for the response function we get the well known the center of gravity method

$$X = \frac{A_x^2}{A_x^1 + A_x^2}$$

$$Y = \frac{A_y^2}{A_y^1 + A_y^2}$$

We use linear approximation for signal corrections

Response function

$$A_i = R(x, y)$$

Reverse response functions give two independent estimates for *X* and two estimates for *Y*

$$X_1 = R^{-1}(A_x^1, A_y^1, A_y^2)$$

$$X_2 = L - R^{-1}(A_x^2, A_y^1, A_y^2)$$

How to evaluate the weighs?

$$X = \frac{X_1 W_1 + X_2 W_2}{W_1 + W_2}$$

Here is the standard approach based on statistical errors

$$W = \frac{1}{\sigma_x^2}$$

…but systematic errors in the response function could be more important → this needs a better understanding

$$\sigma_{x1}^2 = \left(\frac{\partial R^{-1}}{\partial A_x^1}\right)^2 \sigma_A^2$$

$$\sigma_{x2}^2 = \left(\frac{\partial R^{-1}}{\partial A_x^2}\right)^2 \sigma_A^2$$

Evaluating the response functions, R, and inverse response functions, R^{-1}

- Response functions can be directly measured, e.g., using a pulsed laser
- Alternatively, they can be evaluated using iterative fitting process of the experimental data obtained with uncollimated ^{137}Cs source
- As a starting point we use a linear approximation (first order)

Response function is a dependence of the pad signal versus position of the electron cloud

Evaluated response functions (second order approximation)

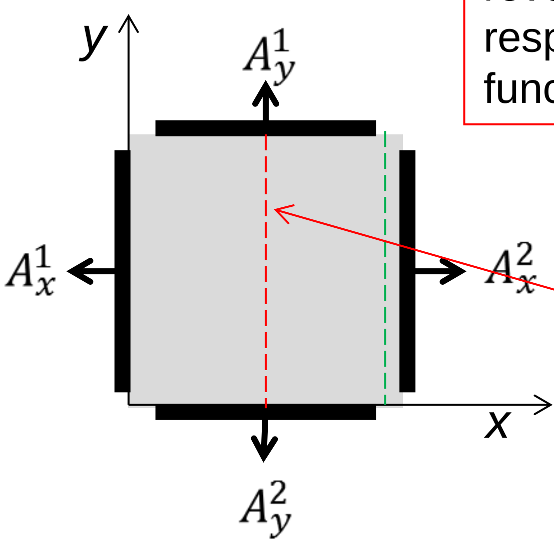

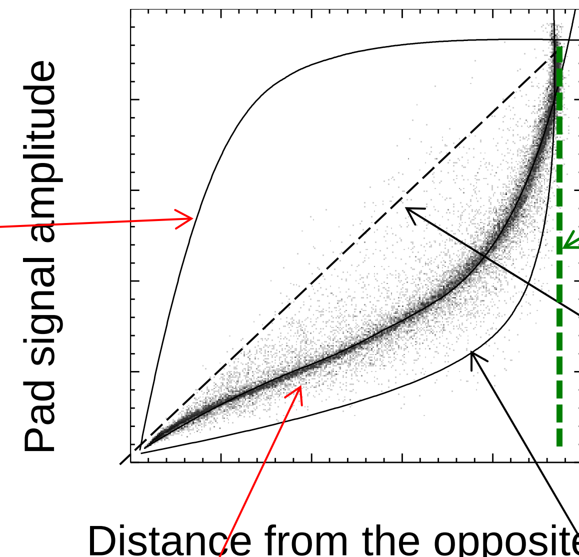

Example of reverse response function

Pad position

Linear approximation

Data points and a fitting curve for a selected narrow region around a center line

Response function near the edges

XY distributions of interaction events measured for a $6x6x20\ mm^3$ detectors using 2-, 3-, and 4- pads readout

Using linear approximation for response functions

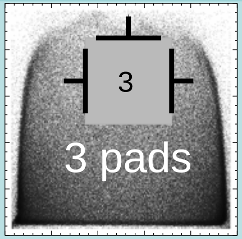

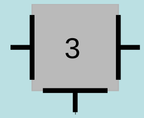

3 pads

3 pads

3 pads

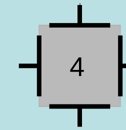

4 pads

9 distributions correspond to different combinations of pad signals

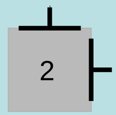

2 pads

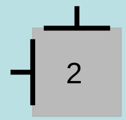

2 pads

2 pads

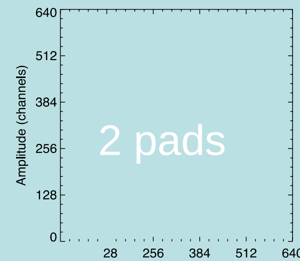

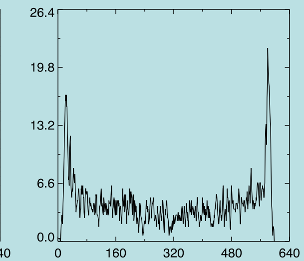

Using the second-order approximation for response functions

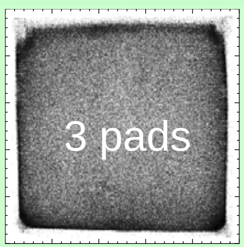

3 pads

3 pads

3 pads

4 pads

2 pads

2 pads

2 pads

2 pads

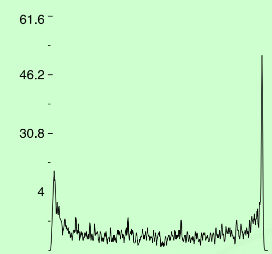

XY response distribution (662-keV photopeak position) measured for a 6x6x20 mm^3 detector using 2-, 3-, and 4-pads readout

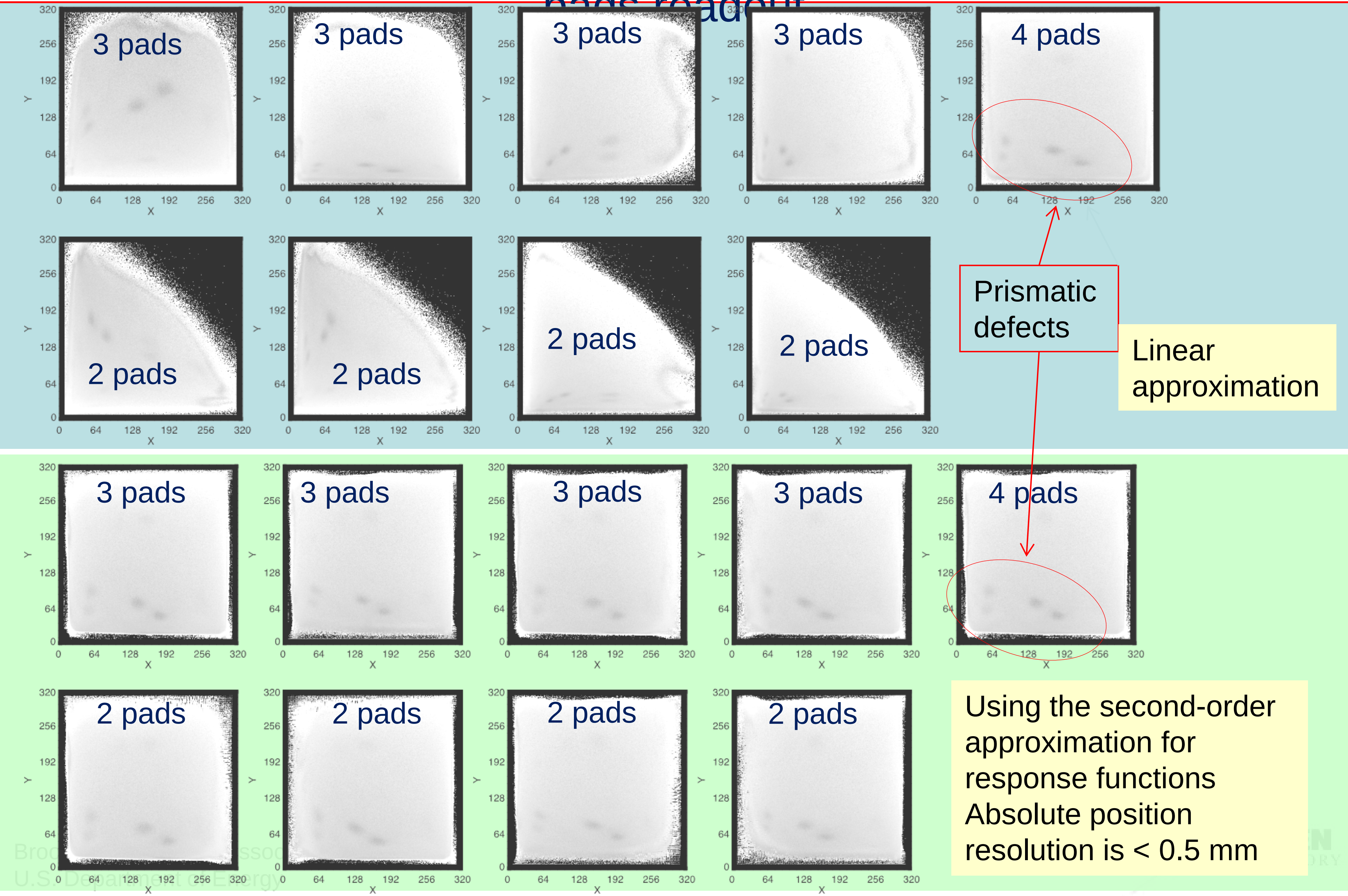

2x2 array modules for the first prototype

Fabricated 2 modules consisting of 2x2 arrays of 20-mm thick detectors

2x2 module layout

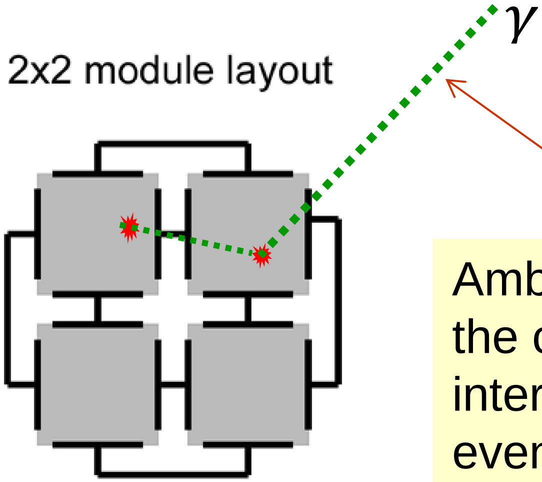

Ambiguity problem in the case on multiple interaction points events

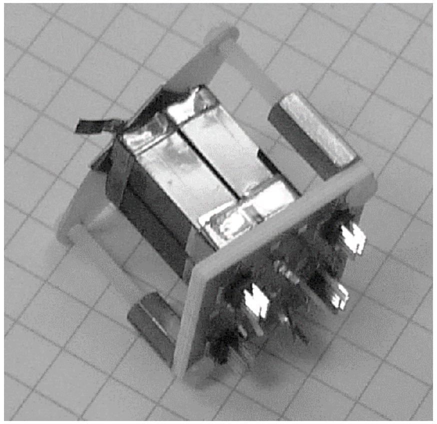

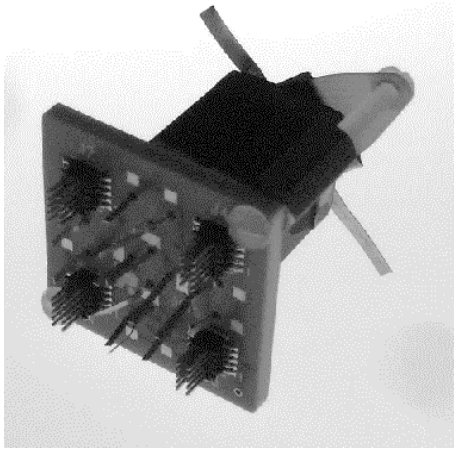

4 anodes
1 common cathode
8 channels for 16 sensing pads
Total: 24 readout channels

As a temporary solution use the existing 36-channel ASIC
The new ASIC is been developed by BNL's Instrumentation

Cs-137 spectra measured with array #1 (6x6x20 mm^3 detectors)

Raw data **After 3D correction**

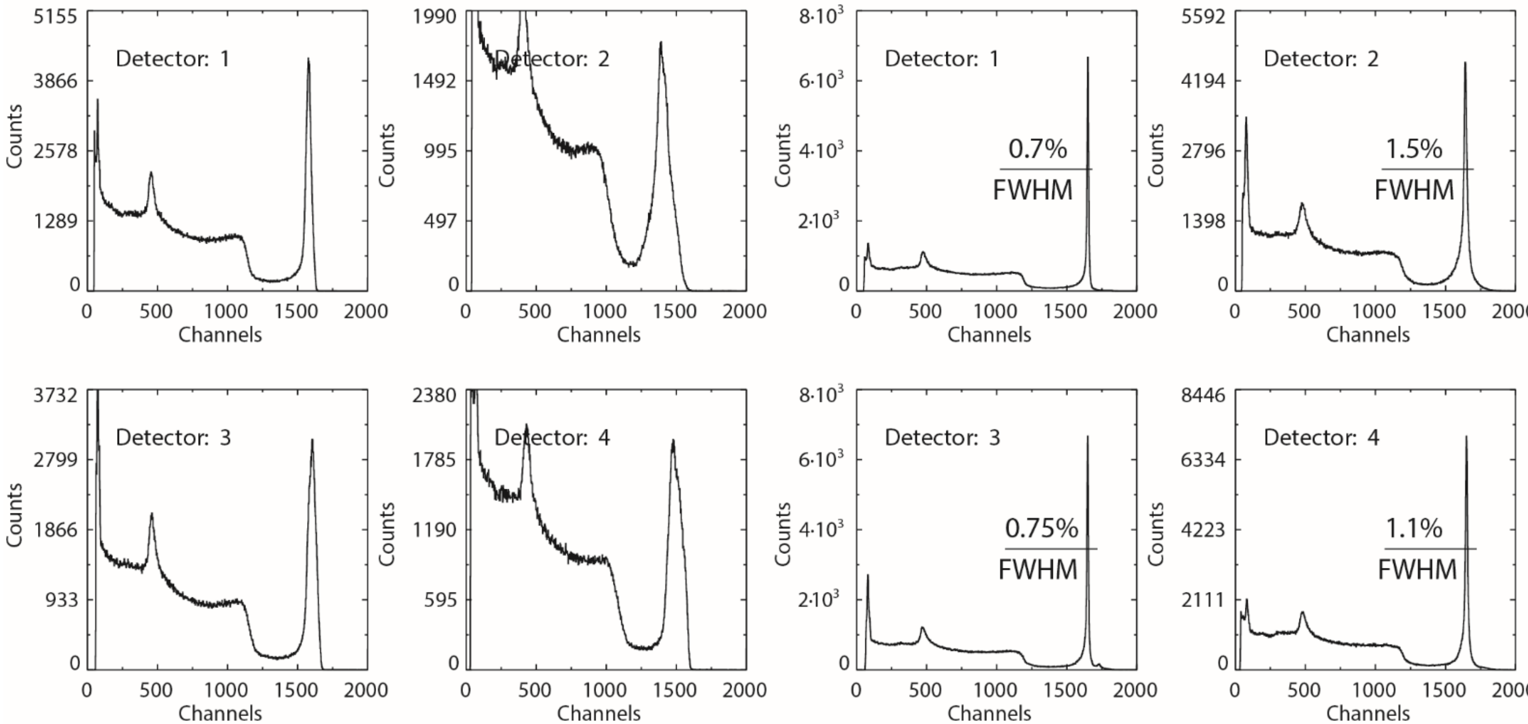

Combined spectrum after corrections

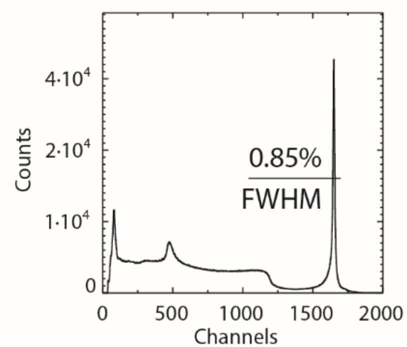

Energy resolution:
0.9% at 662 keV

Cs-137 spectra measured with array #2 (7x7x20 mm^3 detectors)

Raw data

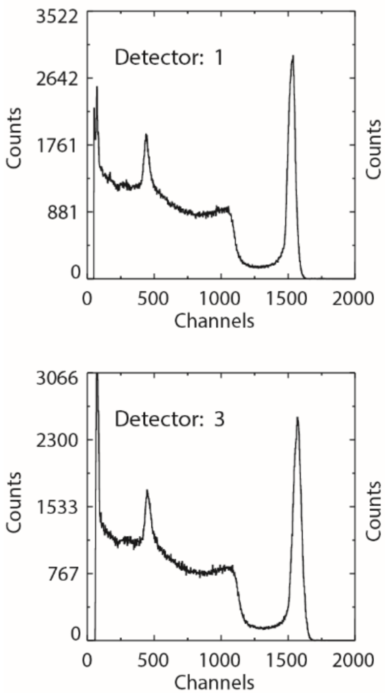

After 3D correction

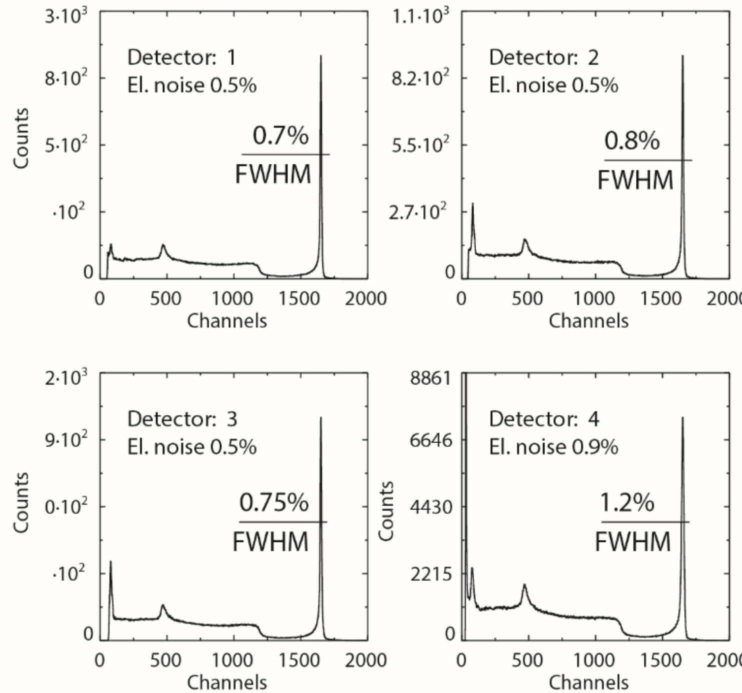

Combined spectrum after corrections

Combined spectrum after corrections

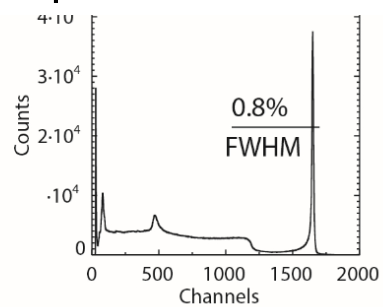

Energy resolution:
0.8% at 662 keV

Response maps (based on photopeak positions) evaluated for the 4 7x7x20 mm^3 detectors before XY corrections

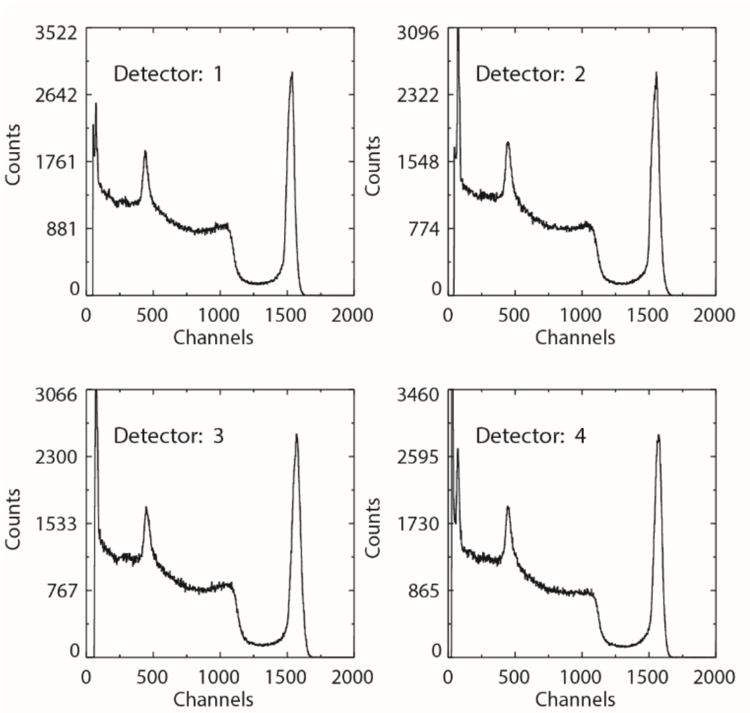

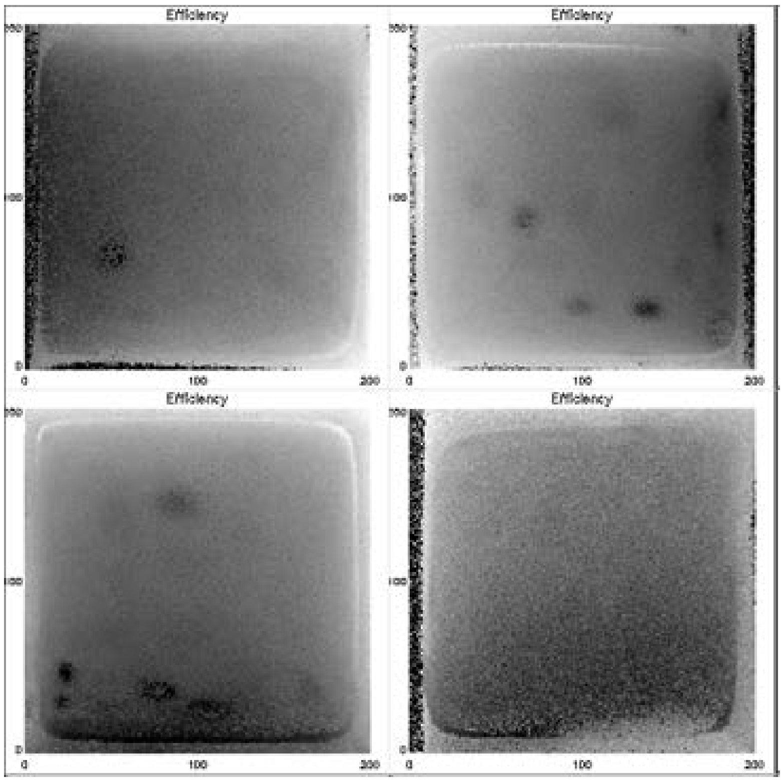

Prismatic dislocations are present in Redlen CZT crystals

Using 2 and 3 pads (instead of 4) to solve ambiguity problem

Raw spectra

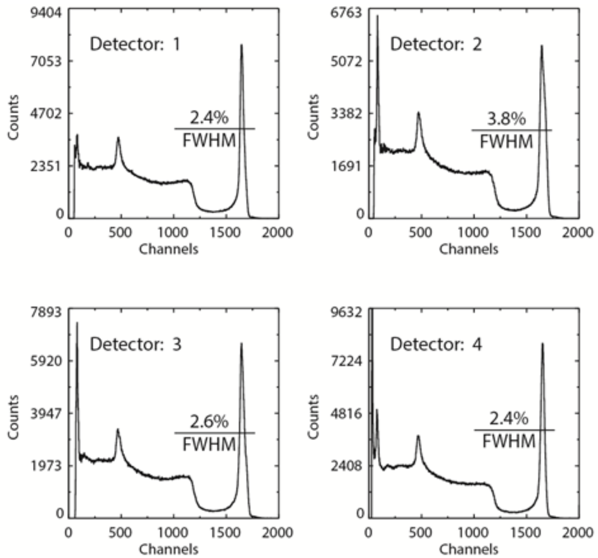

2 pads

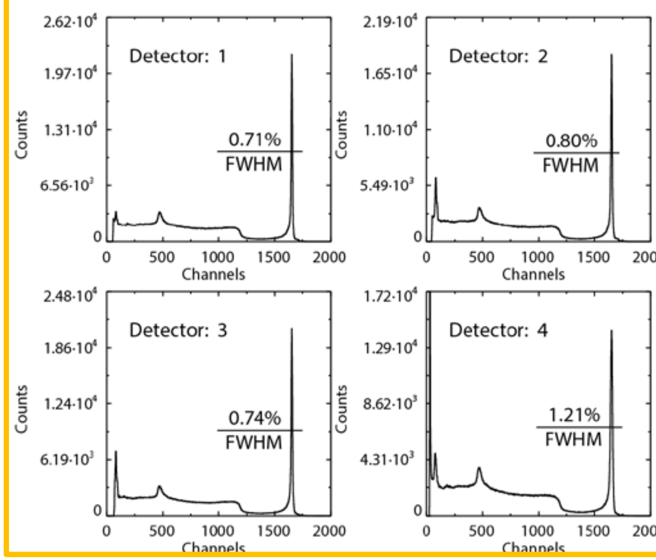

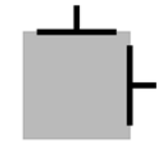

3 pads

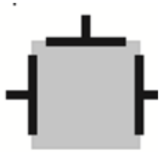

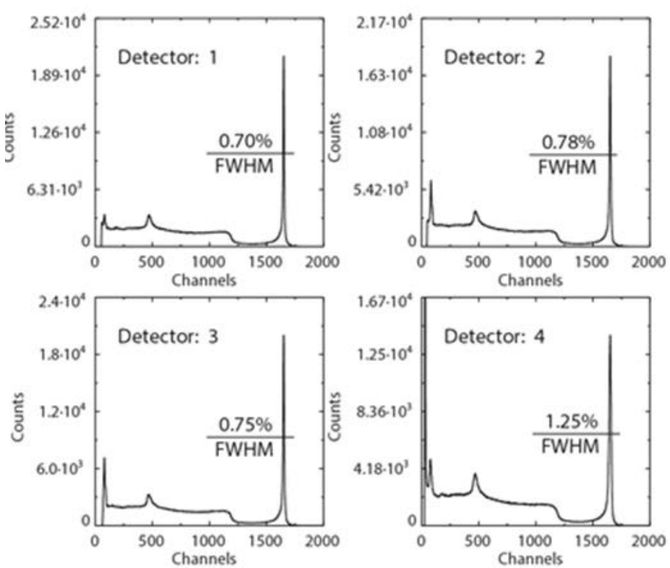

4 pads

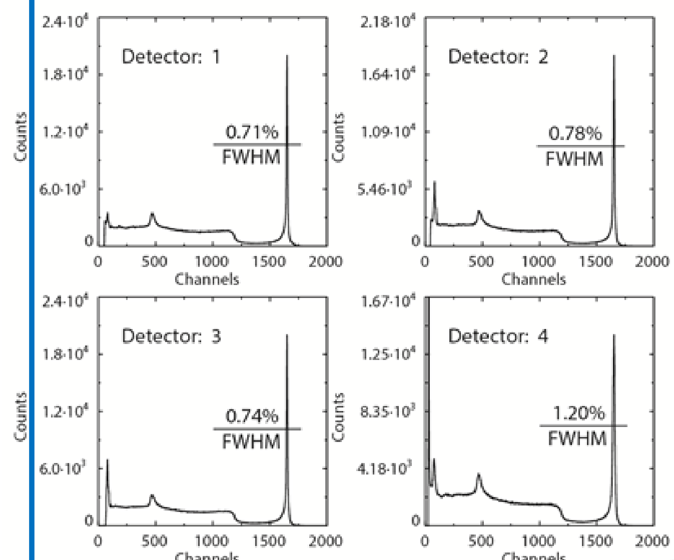

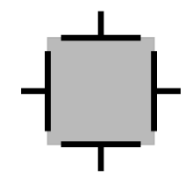

Testing a linear 6-detector array

Linear array of 6 six 5x7x25 mm^3 detectors

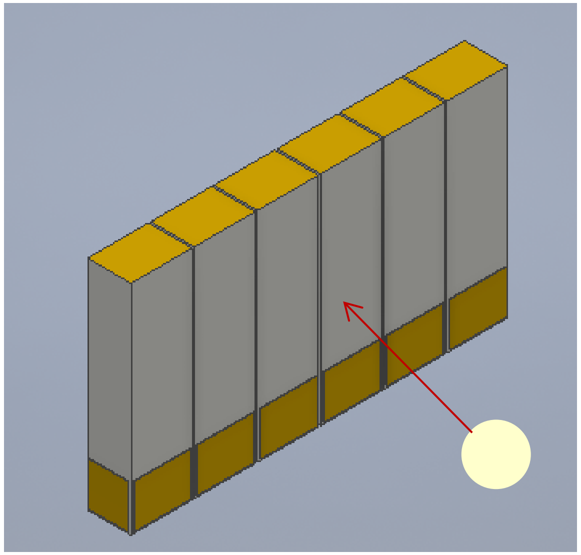

Source from the side

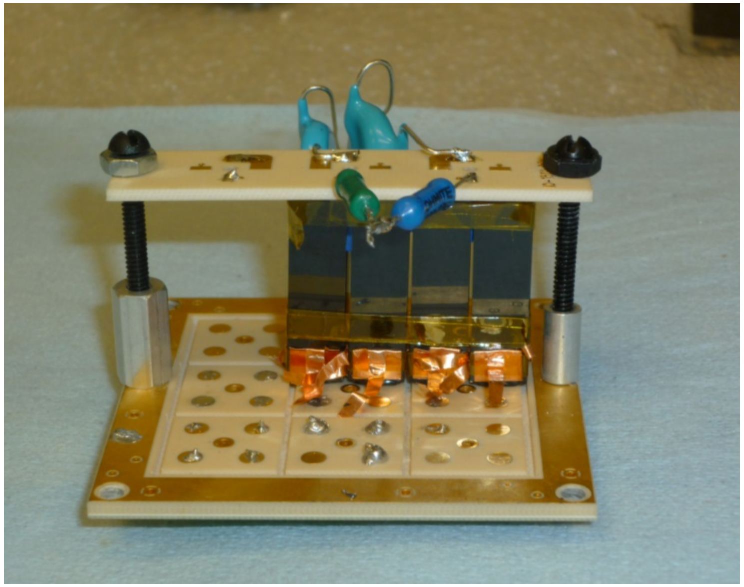

Pulse-height spectra from ^{137}Cs (3500 V)

3D

1D

Raw

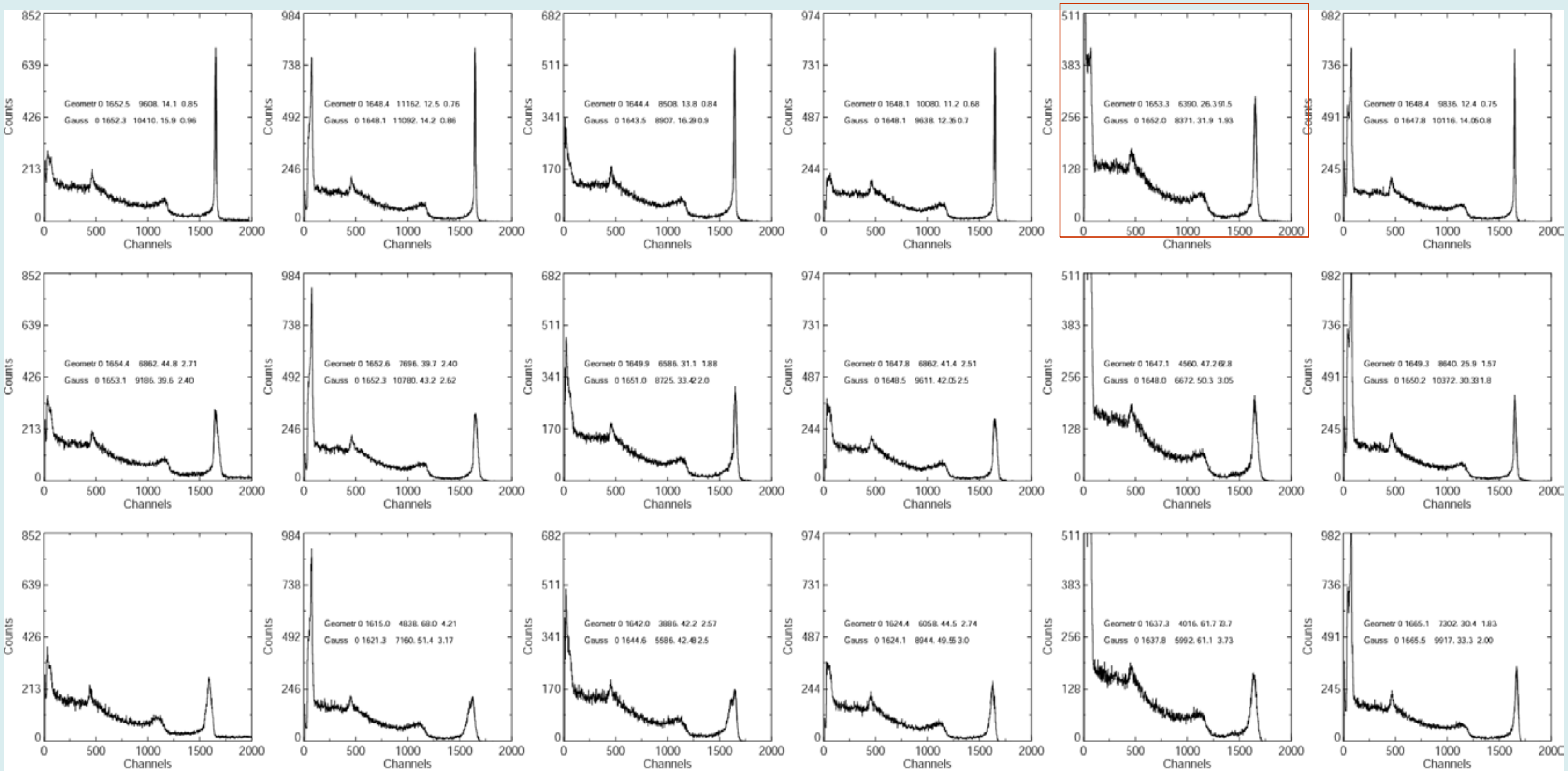

1D corrections
(drift-time corrections)

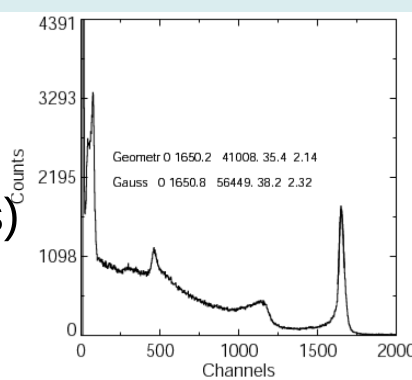

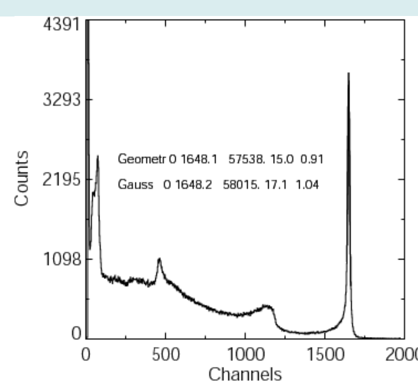

3D corrections

Pulse-height spectra from ^{137}Cs (3500 V)

3D

1D

Raw

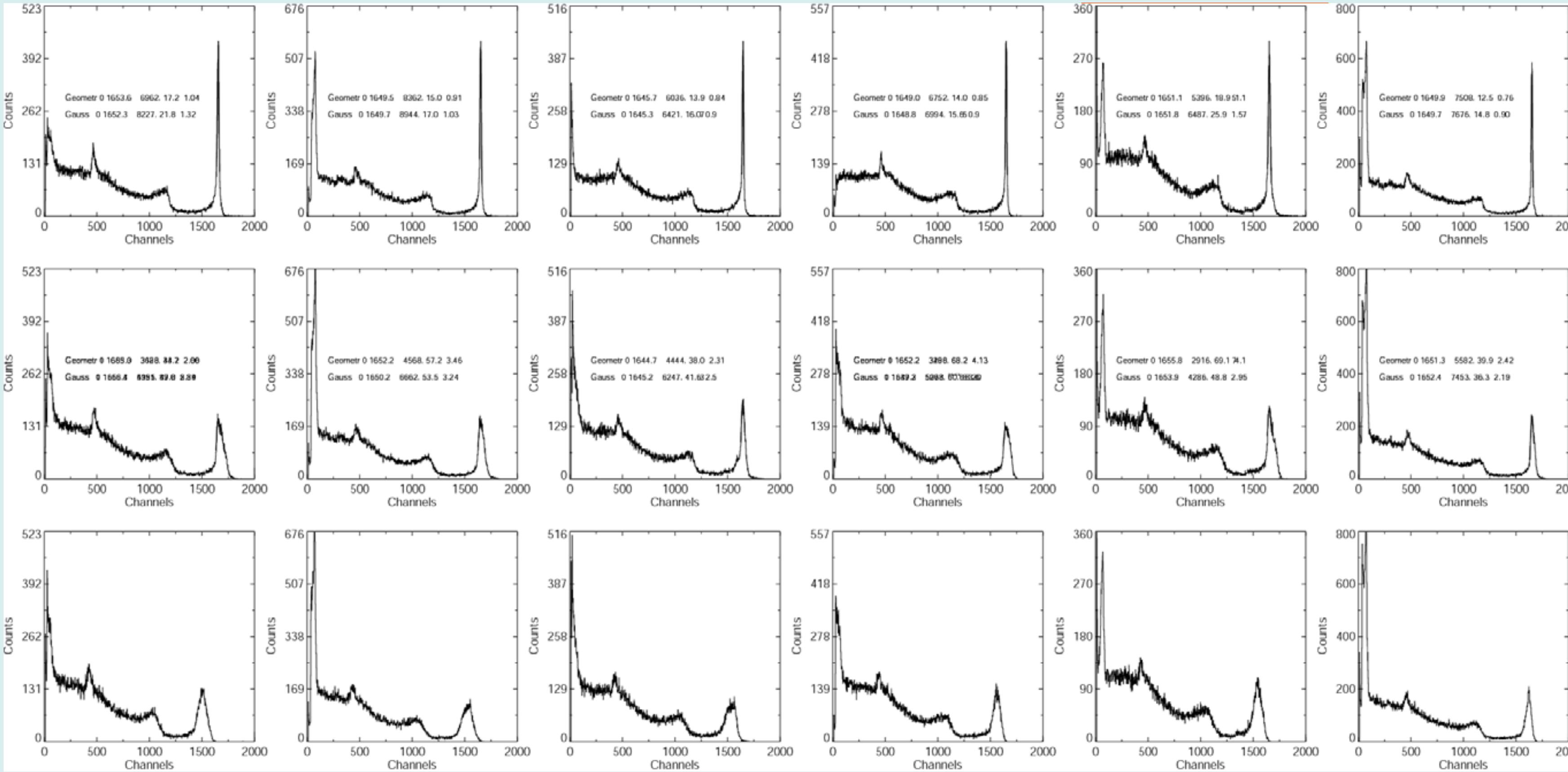

1D corrections
(drift-time correction

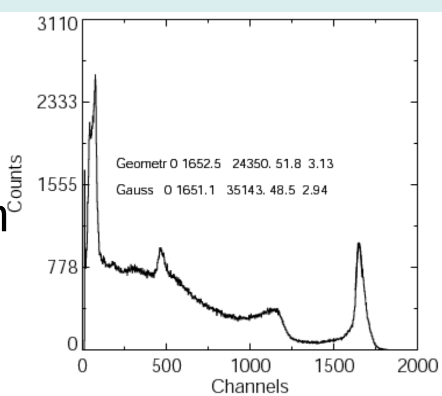

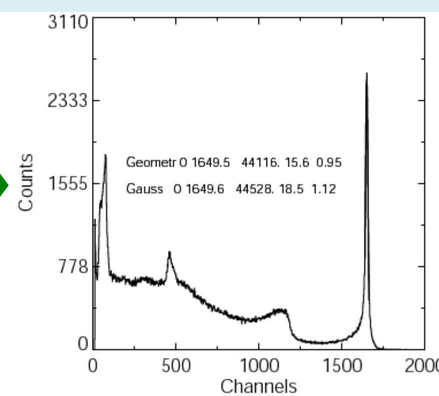

3D corrections

Response maps evaluated for the detectors from the array

Detector 1

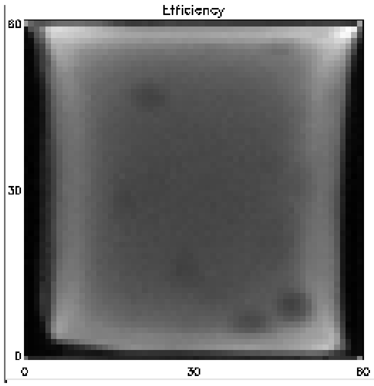

Detector 2

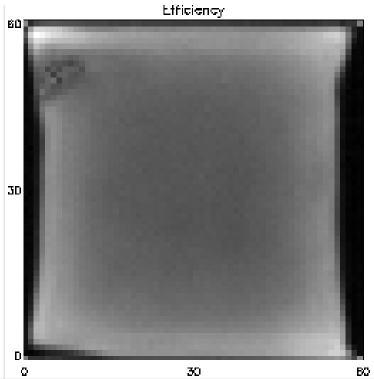

Detector 3

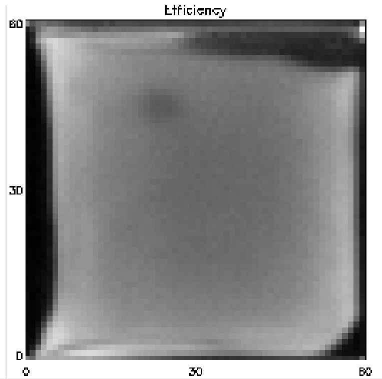

Detector 4

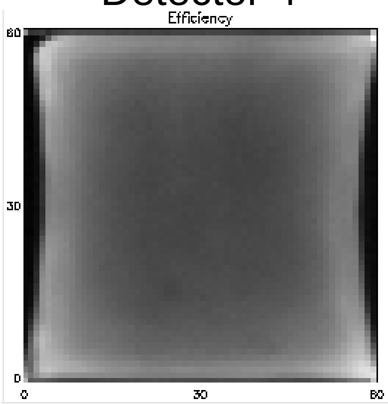

Detector 5

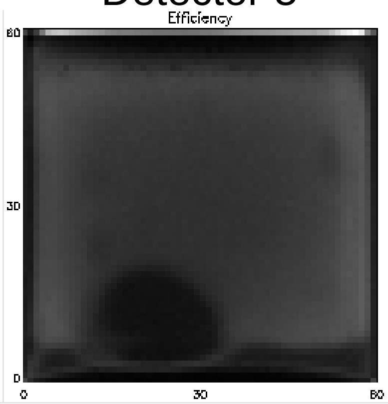

Detector 6

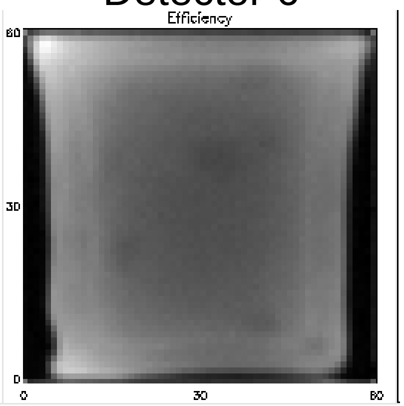

Prismatic dislocations

Pulse-height spectra from ^{134}Cs (2500 V)

3D

1D

Raw

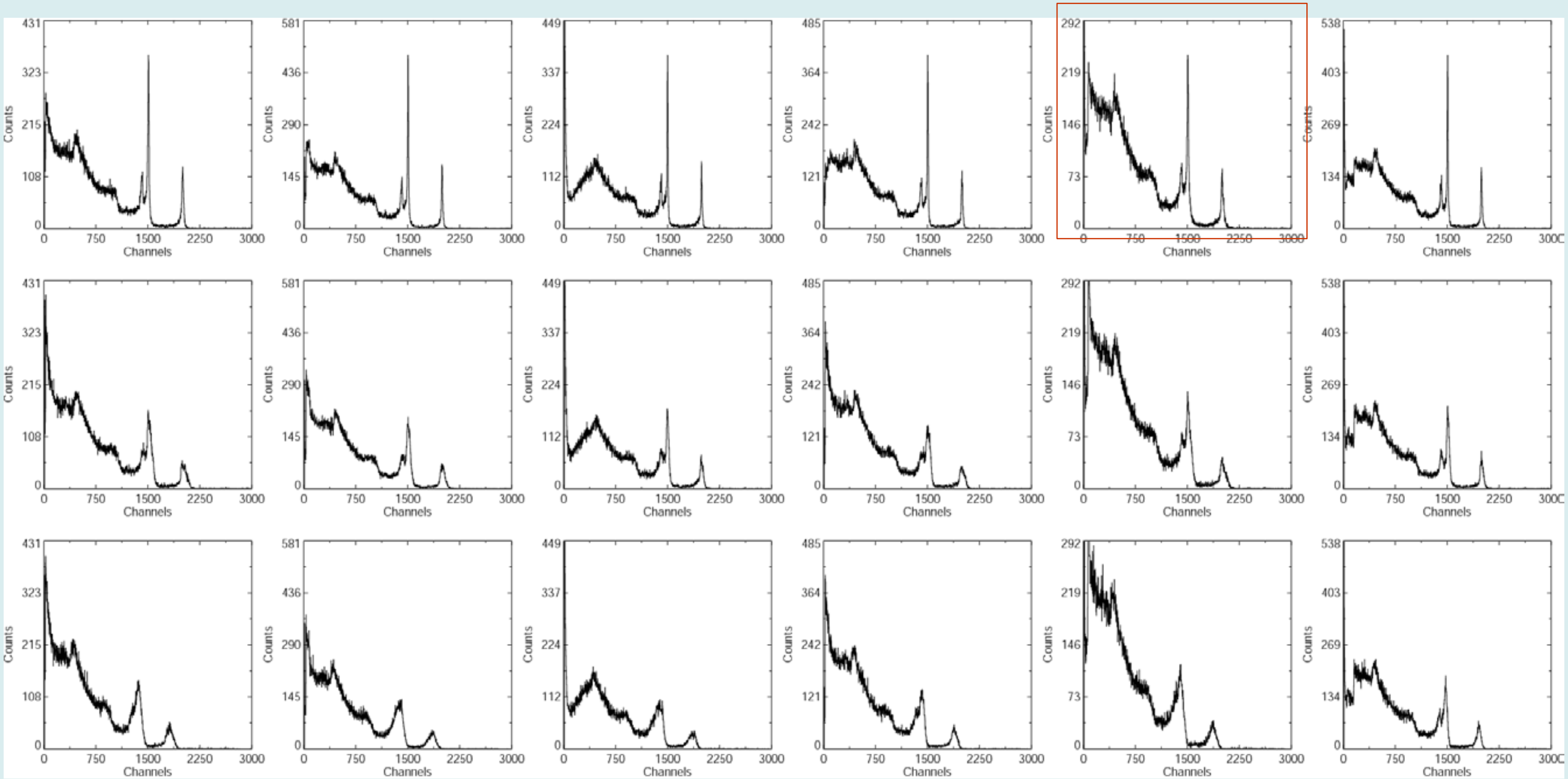

1D corrections
(drift-time corrections)

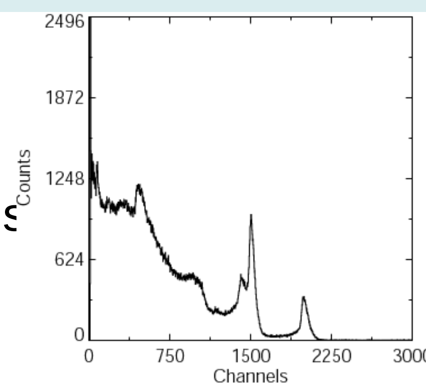

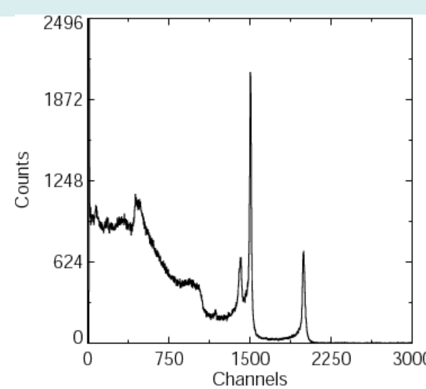

3D corrections

Pulse-height spectra from ^{133}Ba (2500 V)

3D

1D

Raw

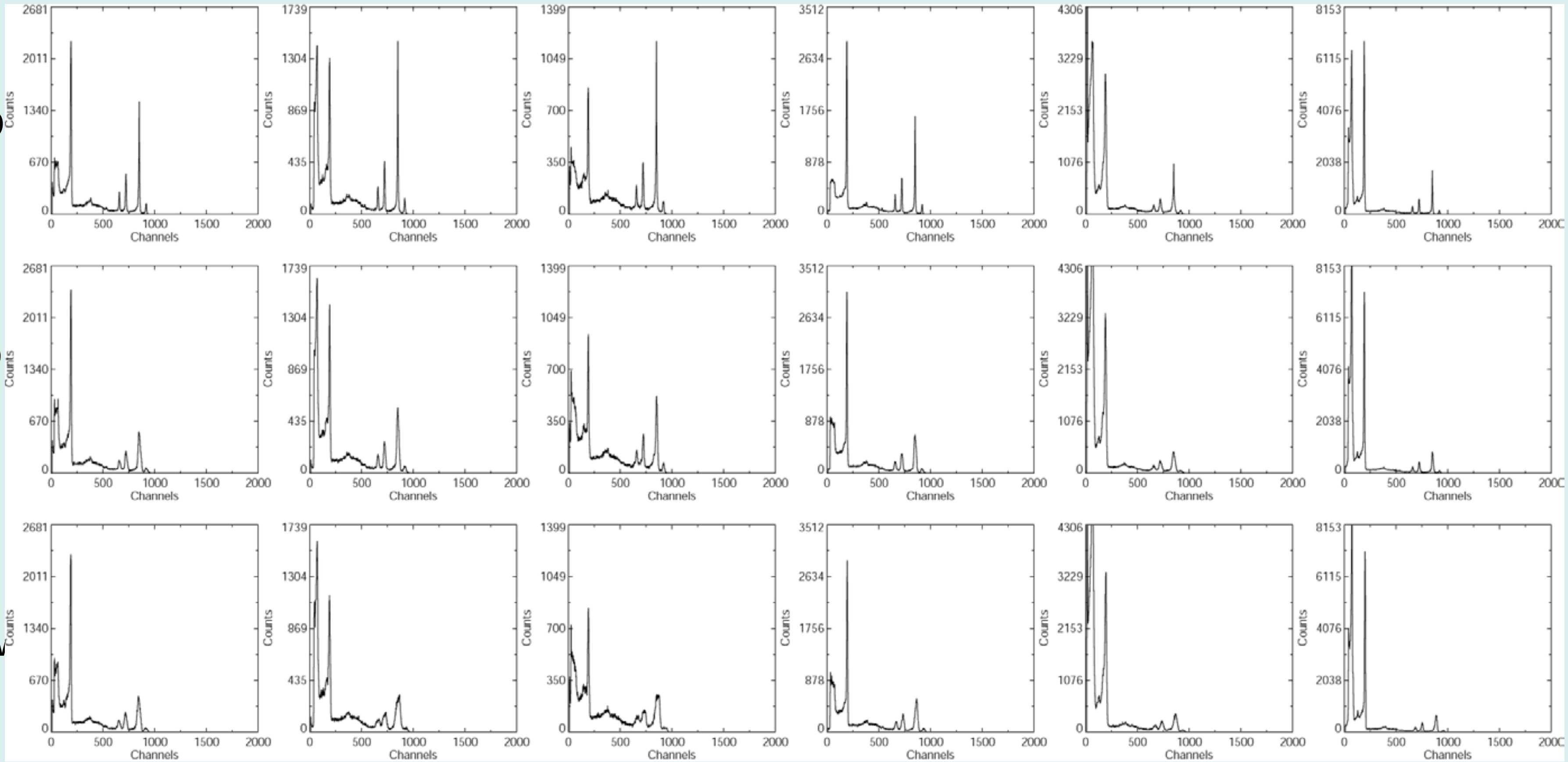

1D corrections
(drift-time corrections)

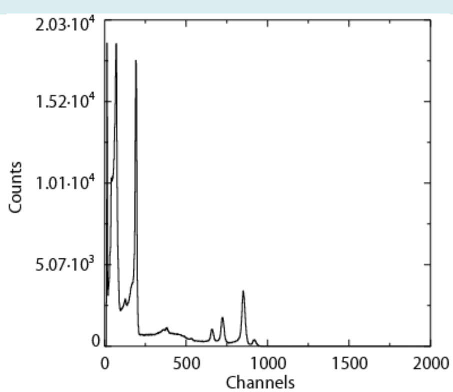

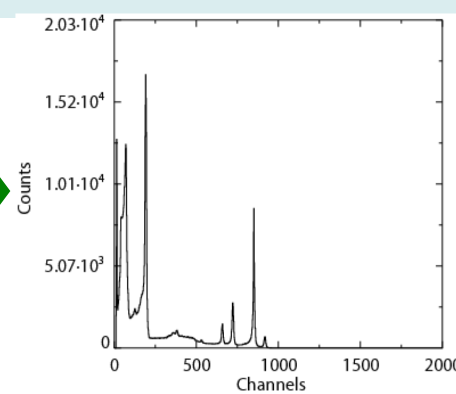

3D corrections

Combined pulse-height spectra of ^{133}Ba (2500 V)

1D

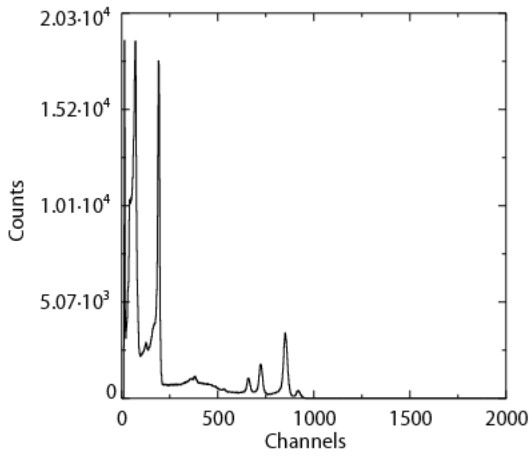

3D

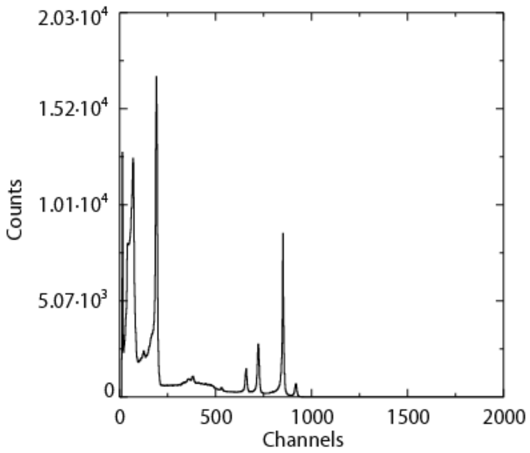

Use a Ba line for calibration

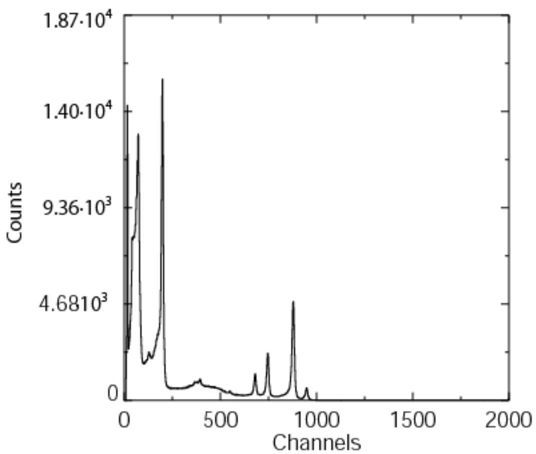

Use a Cs line for calibration

Advantages and drawbacks of the proposed detectors

- Advantages:
  - Large thickness (high efficiency for high-energy gamma rays
  - Good energy and position resolutions
  - Possibility of using standard-grade CZT material (lower cost)
  - Operate at lower HV bias

- Drawbacks:
  - Higher leakage current (electronic noise)
  - Potential polarization in the high gamma-flux conditions (this needs to be tested during the test at SRNL)

Conclusions and future plans

- We demonstrated 2x2 and 1x6 array prototypes of position-sensitive virtual Frisch-grid detectors and readout electronics for a new generation of handheld instruments for safeguard application
- We will perform a demonstration of a measurement of uranium hexafluoride enrichment at SRNL using the lab prototype
- We work with FLIR to incorporate the arrays and new ASIC into the FLIR instrument
- We will demonstrate the FLIR integrated prototype when available

Acknowledgments

The work was supported by the U. S. Department of Energy, Office of Nonproliferation and International Security, Office of Nuclear Safeguards & Security, Next Generation Safeguards Initiative's Safeguards Technology Development Team (NA-241), and Office of Defense Nuclear Nonproliferation Research & Development (NA-22).